AN EXPERIMENT IN MONTE CARLO FORECASTING

A. Hollingsworth

European Centre for Medium Range Weather Forecasts

Abstract

A set of perturbed initial states is generated from a control analysis and used in a Monte-Carlo forecast experiment. The size of the perturbations of the initial state were controlled by the estimated analysis error. The results of the forecast experiment were inconclusive because much of the amplitude of the initial perturbations was removed by the initialisation procedure.

1. INTRODUCTION

There has been much discussion of value in applications of the Monte Carlo approach to stochastic dynamic forecasting, (Leith 1974). However there has been hardly any work published on the application of the method in realistic situations. The present work is one such contribution although the results are inconclusive. In this report we describe an experiment in using the Monte Carlo technique to make stochastic dynamic forecasts with a rather high resolution multi level model. The basic idea was to take an analysis, perturb it within reasonable bounds to produce an ensemble of equally likely initial states from each of the perturbed states and evaluate the results. Section 2 describes the algorithm for perturbing the control analysis, Section 3 describes the model used for the forecasts and Section 4 describes the results.

2. PERTURBATIONS

The analysis system used at ECMWF (Lorenc et al 1977) is based on the statistical interpolation method introduced by Gandin (1963). In addition to analysing the fields the method also provides an estimate of the analysis error. Fig. 1 shows the result of this calculation for 1000 mb and 500 mb height from a typical analysis. The main features - larger analysis errors over the oceans than over land, are quite stable, with the amplitudes showing changes according to the time of year and data coverage.

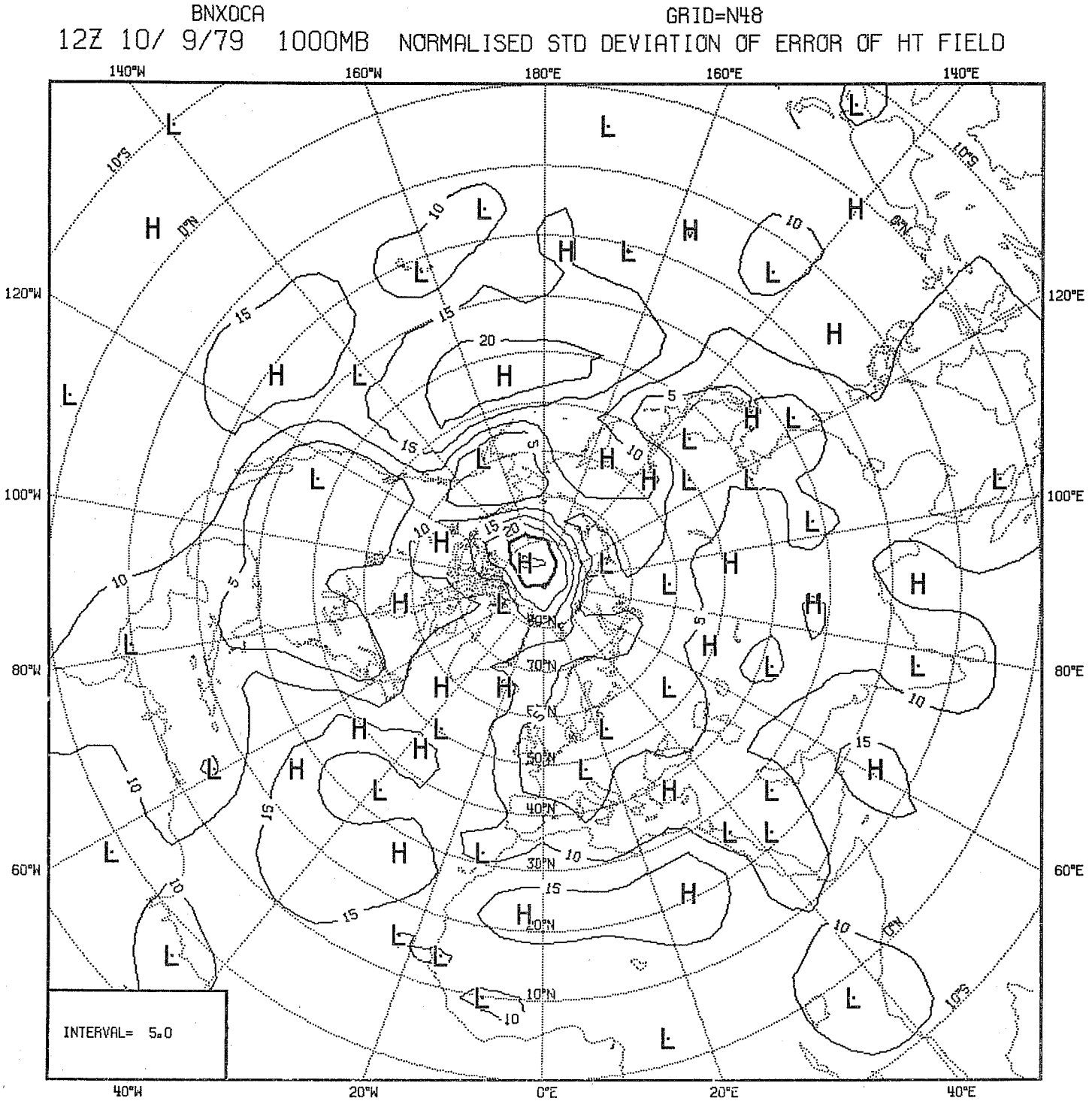

Fig. 1a Normalised standard deviation of analysis error of height field at 1000 mb for 12Z on September 10 1979.

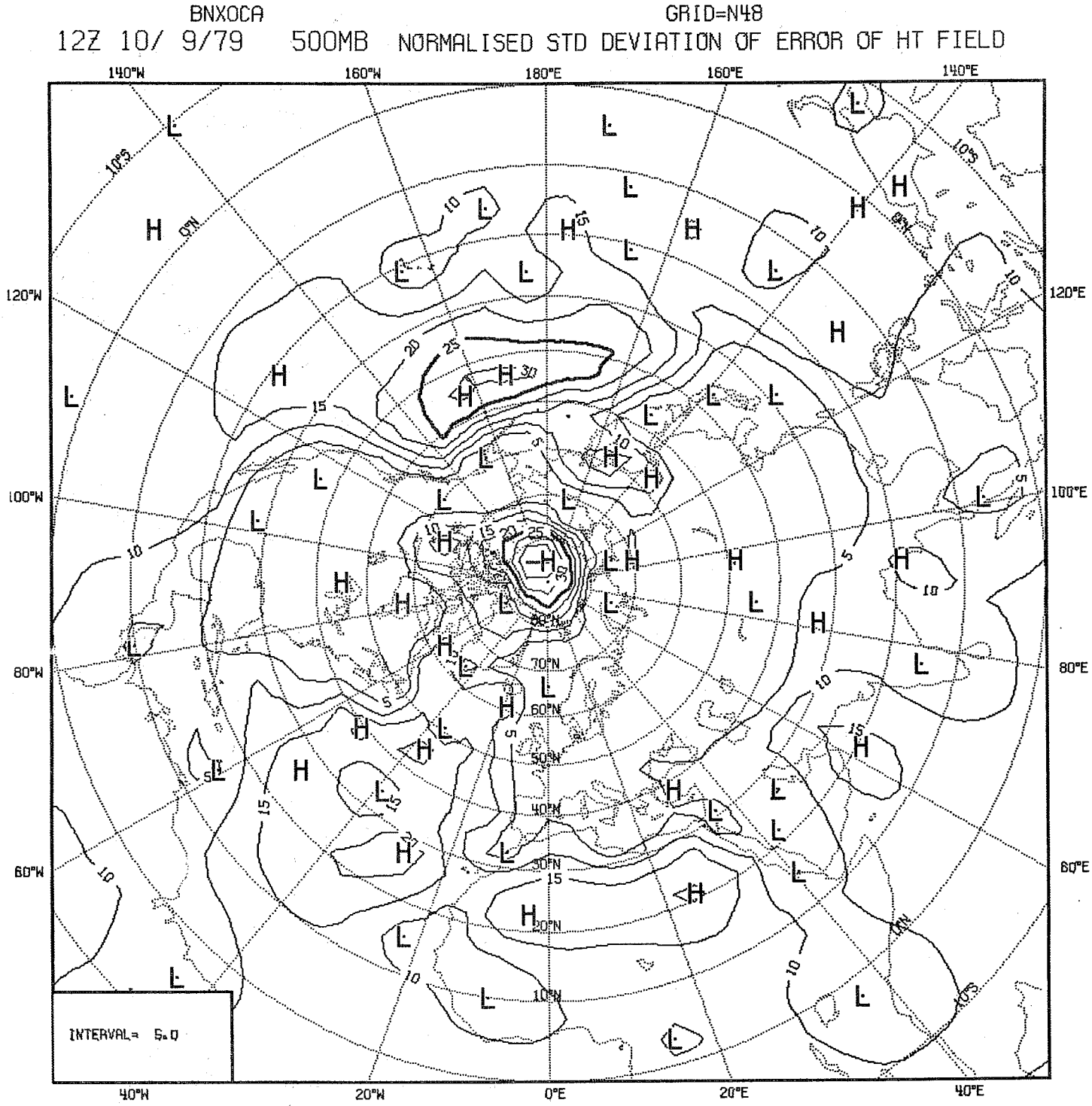

Fig. 1b As Fig. 1a for 500 mb.

We used the analysis error to modulate a random field generated as follows.

The number of grid points at which the global analysis was made was 192 in the east west and 97 in the north south. We generated a similar number of random Fourier sine and cosine coefficients, the coefficients being uniformly distributed in (-1,1). These Fourier coefficients generate a function of the form

$$g'(\lambda,\theta) = \mathrm{Re}\left\{\sum_m \sum_n (a_{mn} + ib_{mn}) \exp(im\lambda + in\theta)\right\} \qquad (1)$$

The randomly generated coefficients were modified so that the mean of (1) was zero and so that all amplitudes were zero for wavelengths less than $6\Delta\lambda$ or $6\Delta\theta$ ($\sim 12^{\circ}$). The amplitudes were further modified near the poles such that no scales were included whose physical wavelength was less than the zonal two grid length wave at 45°.

The expression (1) was used to evaluate g' north of 10° north with g' being set to zero south of this latitude. Within 6 grid lengths of the pole the field of g' was multiplied by $\frac{\cos\theta}{\cos(\pi/2 - 6\Delta\theta)}$ to smooth the polar field, and south of 45 N g was multiplied by $\frac{\sin\theta}{\sin 45}$ to taper off the perturbation field towards the equator. Finally we scaled g' to have mean zero and standard deviation 1 on the northern hemisphere.

The initial data we worked with were the operational analysis for September 10, 1979.

To get the perturbation of geopotential we multiplied the calculated height analysis error by the random function g' described above. The analysis error varied with height but we used the same g' at each level in order not to introduce static instability into the system. Thus

$$\phi'(\lambda,\theta,p) = E_{\phi}(\lambda,\theta,p) * g'(\lambda,\theta)$$

where ϕ' is the perturbation in the geopotential and E_{ϕ} is the analysis error in geopotential. We then calculated geostrophic winds corresponding to the height perturbation and added the

velocity and height perturbations to the control analysis. The purpose in this was to provide perturbations of the meteorological modes which would hopefully survive the nonlinear normal mode initialisation procedure.

After the perturbation fields were added to the control analysis, the resulting fields were interpolated to σ-coordinates and initialised using the non linear normal mode initialisation technique (Temperton and Williamson 1979).

Fig. 2 shows a typical perturbation in the 500 mb height field before initialisation. The amplitudes are largest over the oceans and smaller over the continents as expected. The smallest scale of the perturbations is of the order of 1000 km. We generated four such perturbation fields. Visual inspection revealed very little resemblance between them apart from the land-sea differences already noted. However very little of this smaller scale structure survived the initialisation. Fig. 3 shows the mean 500 mb geopotential difference between the control analysis and the perturbed states while Fig. 4 shows the variance at 500 mb of the initialised perturbations about the mean. It is clear that apart from the polar regions all the perturbed states are nearly the same. The mean of the perturbations reaches 90 m in places while the sample variance is at most 10 m in mid latitudes. We do not understand the reasons for this result. In principle the perturbations should have survived since we prescribed them to be geostrophic. This is a serious limitation of the present work.

An alternative approach that should be investigated is to add the perturbations to a state at rest, initialise the resulting states and then add these initialised perturbations to the initialised control analysis. In such a case the non linear corrections would be quite small and it is presumably the non linearity which is reducing the variance in the perturbation fields.

At any rate, since the initialised perturbed states show little variance within the sample the results of the forecast experiments described in Section 4 are not too surprising.

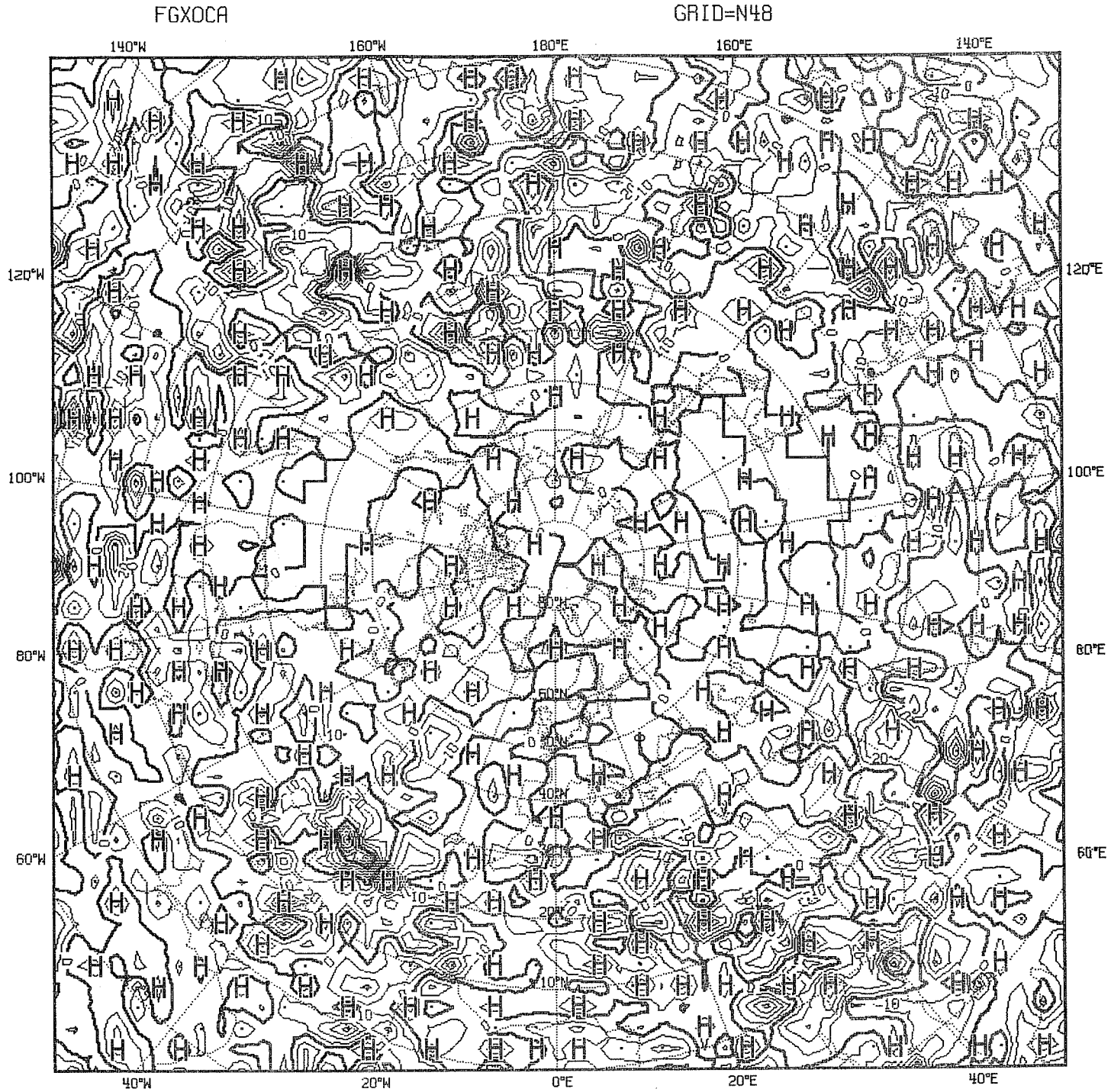

Fig. 2 Example of a perturbation geopotential height field at 500 mb.Contour interval 10 m.

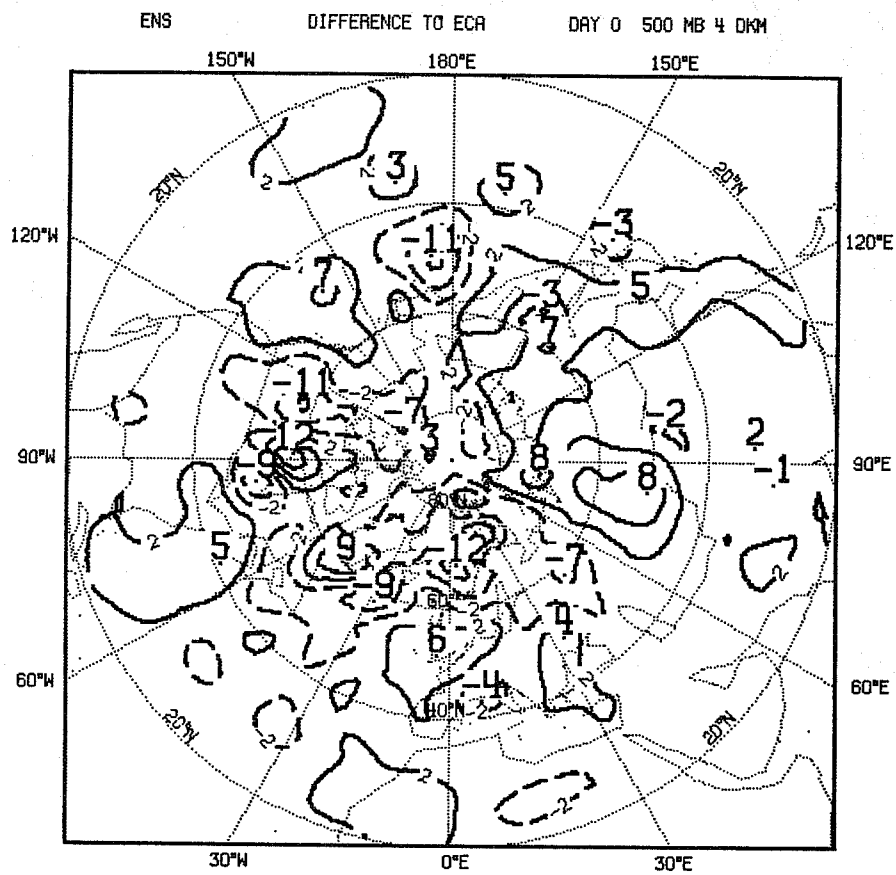

Fig. 3 Difference between the initialised 500 mb fields of the ensemble mean of the perturbed initial states and the control analysis. The interval is 4 dam starting at ± 2 dam.

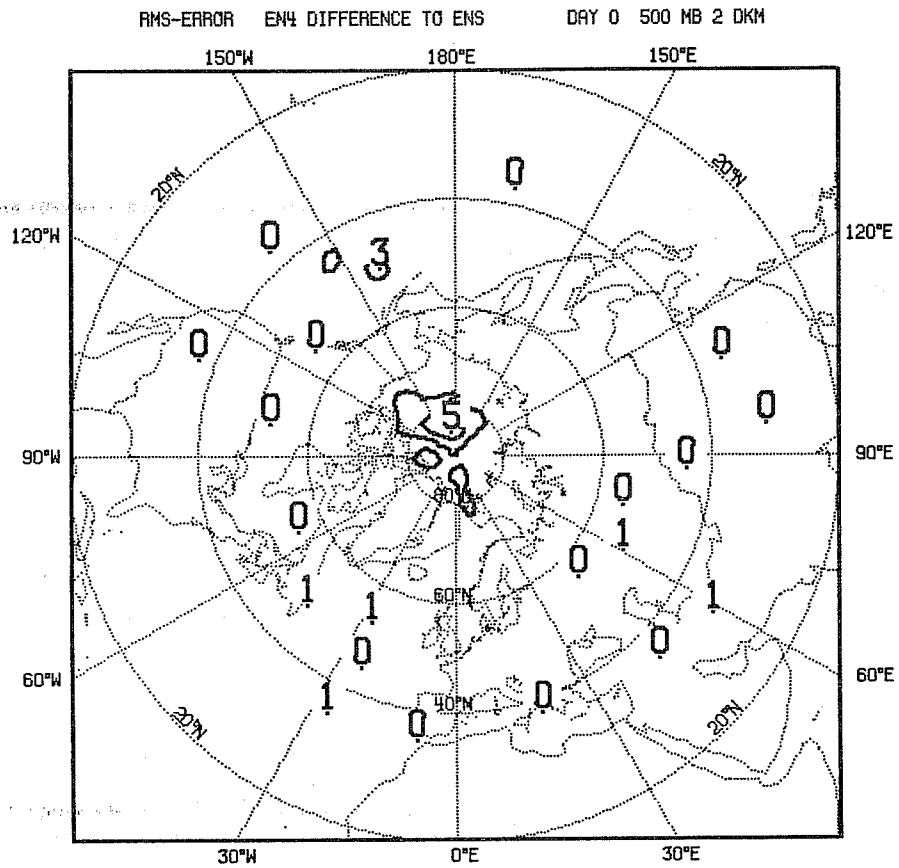

Fig. 4 Standard deviations of the initialised 500 mb height field within the sample of four perturbed states.

3. FORECAST MODEL

After initialisation by the grid point model the data was interpolated to a gaussian grid and the fields fitted with a triangular-40 spherical harmonic representation. The forecasts were made with a spectral model using this resolution in the horizontal and fifteen levels in the vertical (Baede et al 1978). The physical parameterisation was that used in the ECMWF operational model (Tiedtke et al 1979). The time scheme was semi-implicit with a step of 40 min so that a ten-day forecast took just under 1 hour of CP time. Experience shows that initialisation using the grid point model produces satisfactory integrations in the spectral model.

4. RESULTS

As one would expect the rate at which the individual forecasts (within the ensemble of perturbed forecasts) deviated from each other was quite slow. What was more surprising was the fact that the ensemble mean of the forecasts also deviated from the control forecast rather slowly. Figs. 5-7 show the verifying analysis, the control forecast and the ensemble mean of the perturbed forecasts at 500 mb for days 4,7,10. The initial data, it should be said, was chosen because it was one for which the control forecast was not very good. This allowed the possibility that a rapid growth of difference between the perturbed forecasts would indicate areas where the control forecast was unreliable. Synoptically there is very little to choose between the ensemble mean forecast and the control forecast. Both forecasts have the same failure in over-developing the trough over western Europe. Even at day 7 the control and the ensemble mean forecasts are quite similar in most areas. The only exception is the region around Labrador where the control forecast shows an active development. The perturbed forecasts disagreed with each other and with the control in this region and so the ensemble mean shows a fairly slack flow in this region. By day ten the control forecast has lost predictive skill in most features. The only one which seems to have been forecast at all successfully is the ridge around 80 E and interestingly enough the ensemble mean forecast also shows this feature.

Figs. 8-10 show the distribution of variance in 500 mb height within the ensemble at days 4,7,10. Between days 0 and 4 there is very little growth in the sample variance but thereafter the growth is more rapid.

Fig. 11 shows the time evolution of the RMS errors for both control and the ensemble mean forecasts (averaged over the northern hemisphere north of 20 N and below 200 mb). The ensemble mean shows a slightly better RMS score but this could easily occur merely because the ensemble mean flow has less variance. On the other hand two of the members of the ensemble did have better scores than the control. Fig. 12 shows the time evolution of the anomaly correlation coefficient for the same region and here too the ensemble mean shows a slightly better score. Figs. 13 and 14 show the time evolution of the growth of difference between the control and the ensemble mean forecasts. The differences grow very slowly in time and are much slower in growth than was found between running two models which differed only in their physical parameterisations (Hollingsworth et al 1979).

5. CONCLUSIONS

The results of these experiments are inconclusive because of the difficulty that was experienced in having the initial geostrophic perturbations survive the initialisation procedures. Further work must be undertaken to overcome this problem.

References

Leith, C.E. 1974 Theoretical skill of Monte Carlo forecasts. Monthly Weather Review, 10 409-418

Lorenc, A. et al 1974 The ECMWF analysis and data-assimilation scheme. Analysis of Mass and Wind fields. ECMWF Tech. Report No. 6

Gandin, L.S. 1963 Objective analysis of meteorological fields. Leningrad

Temperton, C. and D Williamson 1979 Normal mode initialisation for a multi-level grid point model. ECMWF Tech. Report No.11

Baede, A.P.M. et al 1978 Documentation of the ECMWF spectral model ECMWF Internal Report No.10

Tiedtke, M. et al 1979 ECMWF Model - Parameterisation of sub-grid scale processes. ECMWF Tech. Report No.10

Hollingsworth, A. et al 1979 Comparison of medium range forecasts made with two parameterization schemes. ECMWF Techn. Report No.13

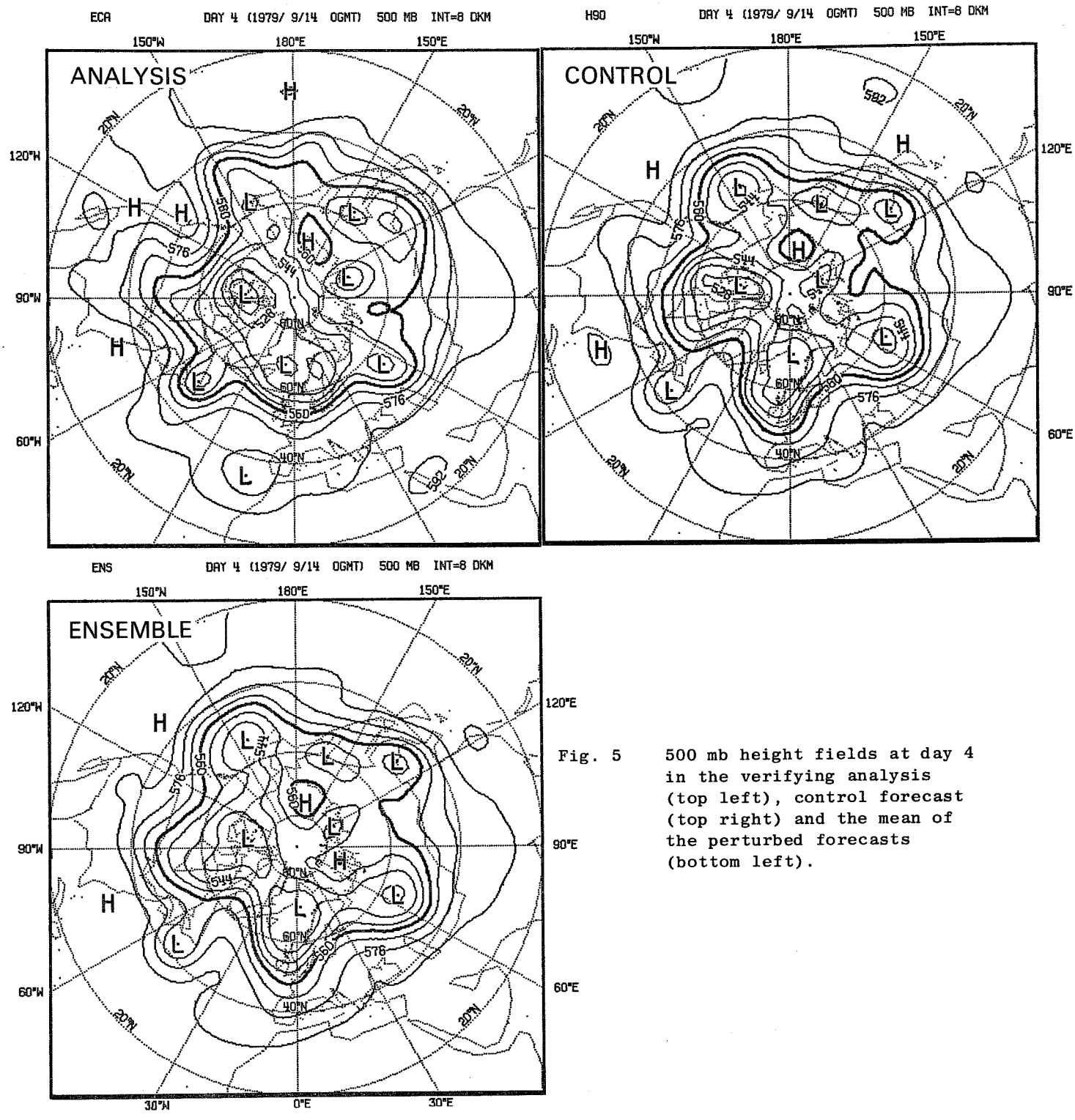

Fig. 5 500 mb height fields at day 4 in the verifying analysis (top left), control forecast (top right) and the mean of the perturbed forecasts (bottom left).

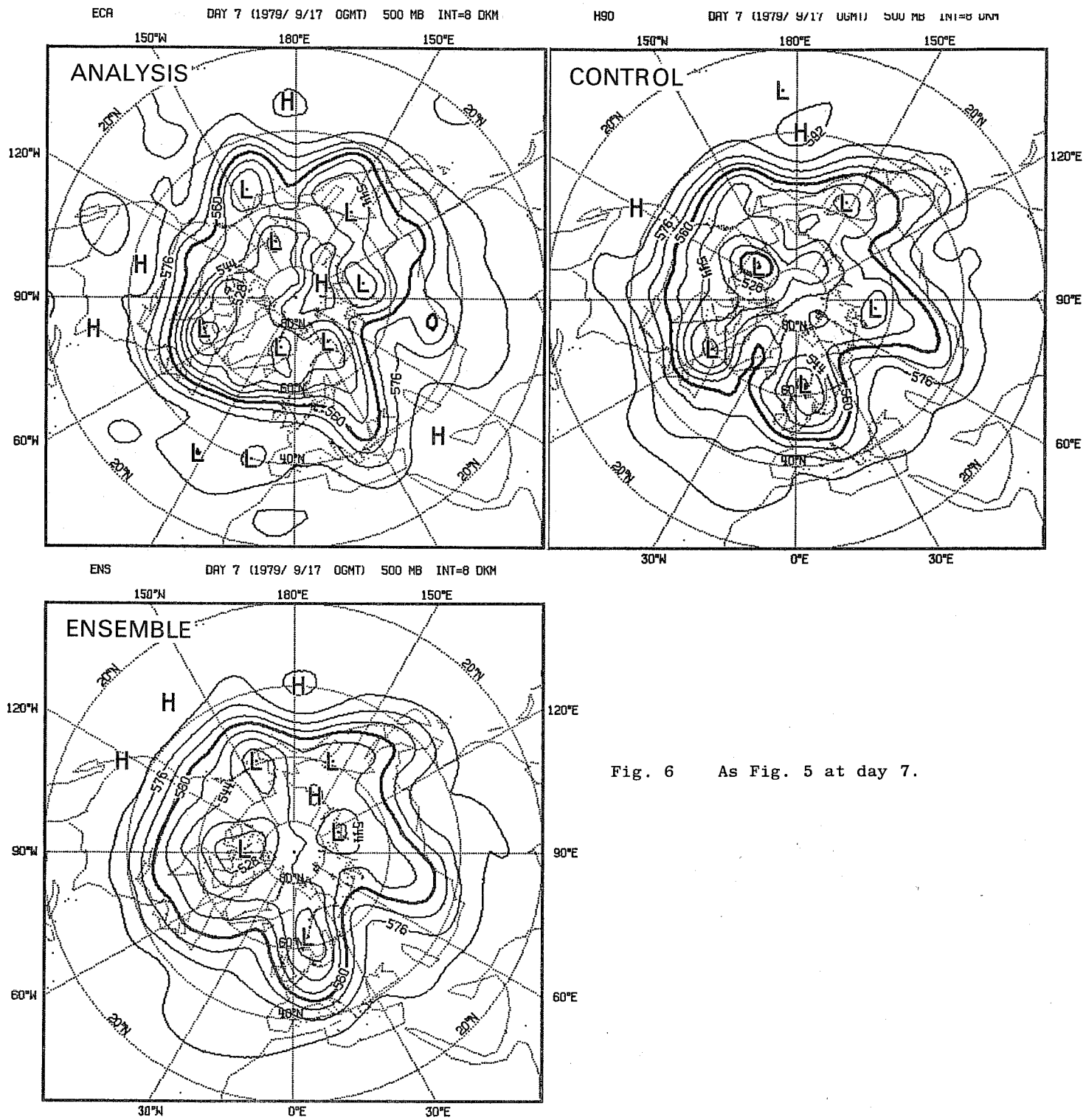

Fig. 6 As Fig. 5 at day 7.

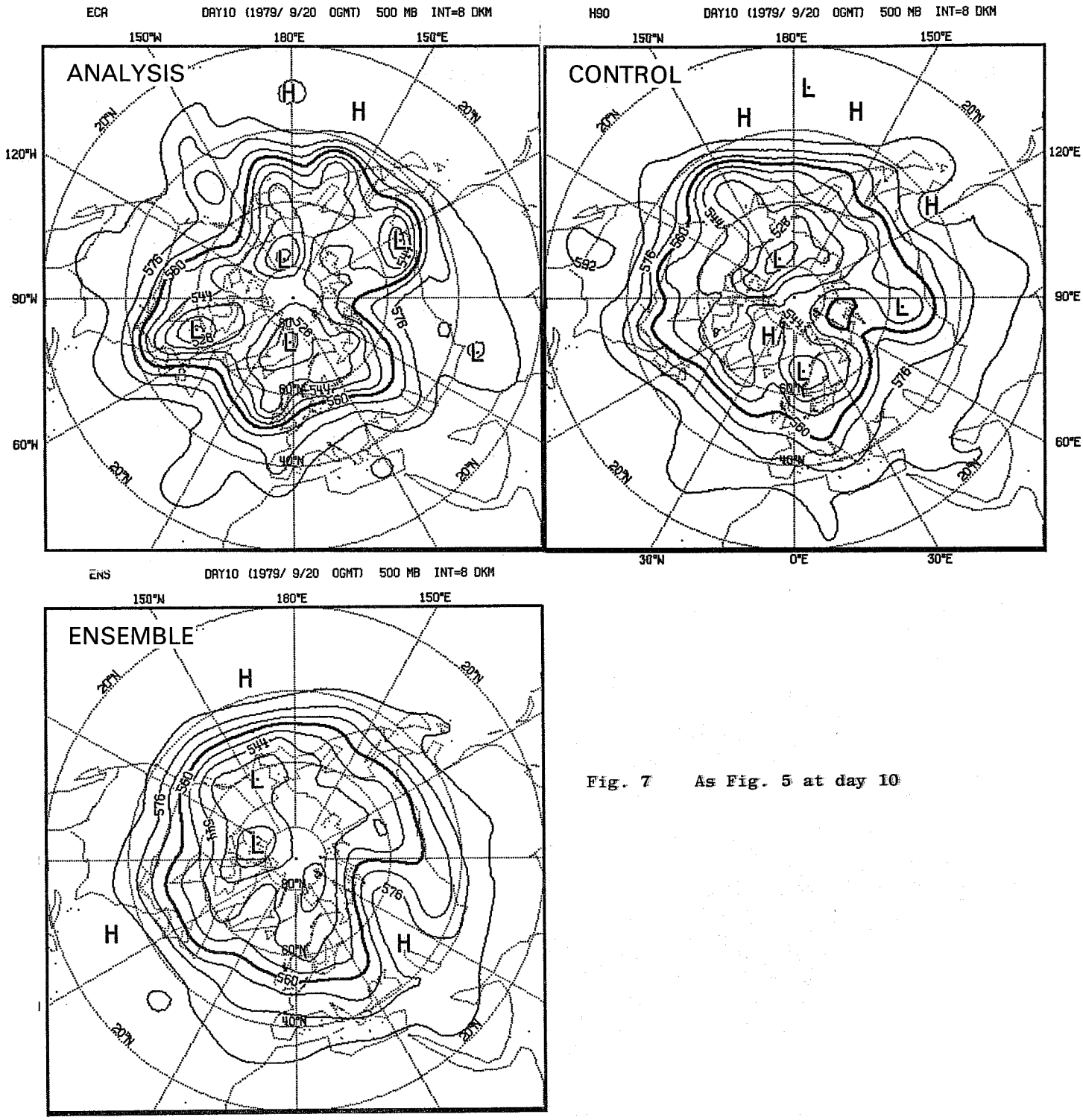

Fig. 7 As Fig. 5 at day 10

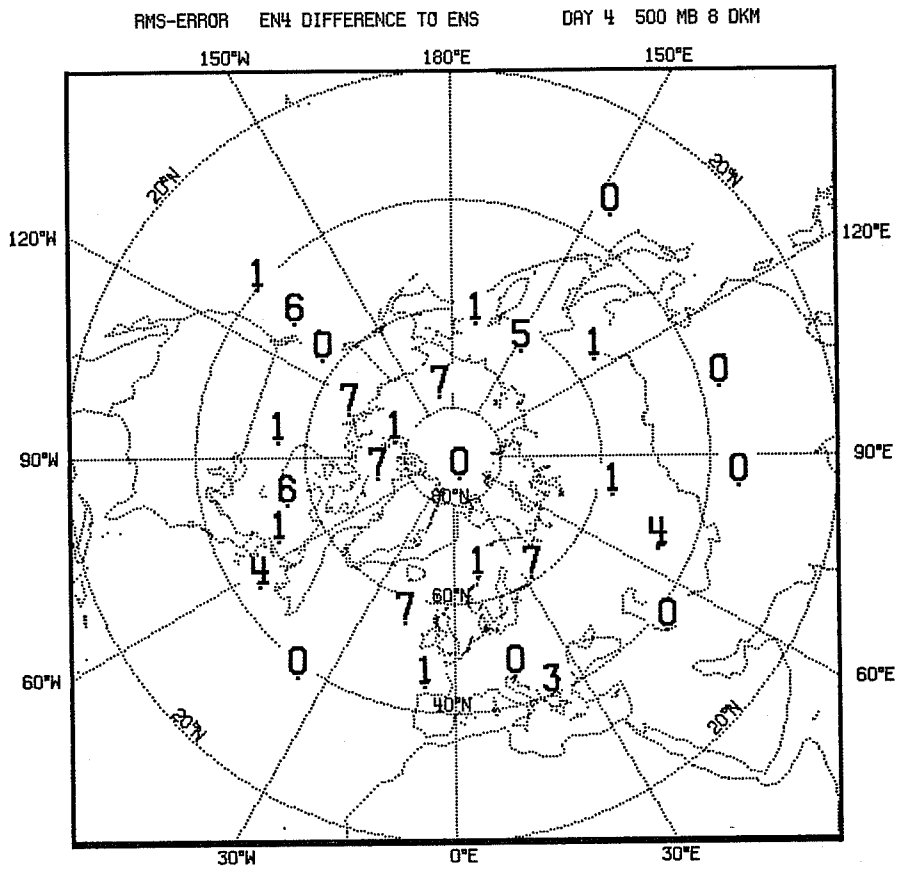

Fig. 8 Standard deviation of the 500 mb height field in the set of four perturbed forecasts at day 4.

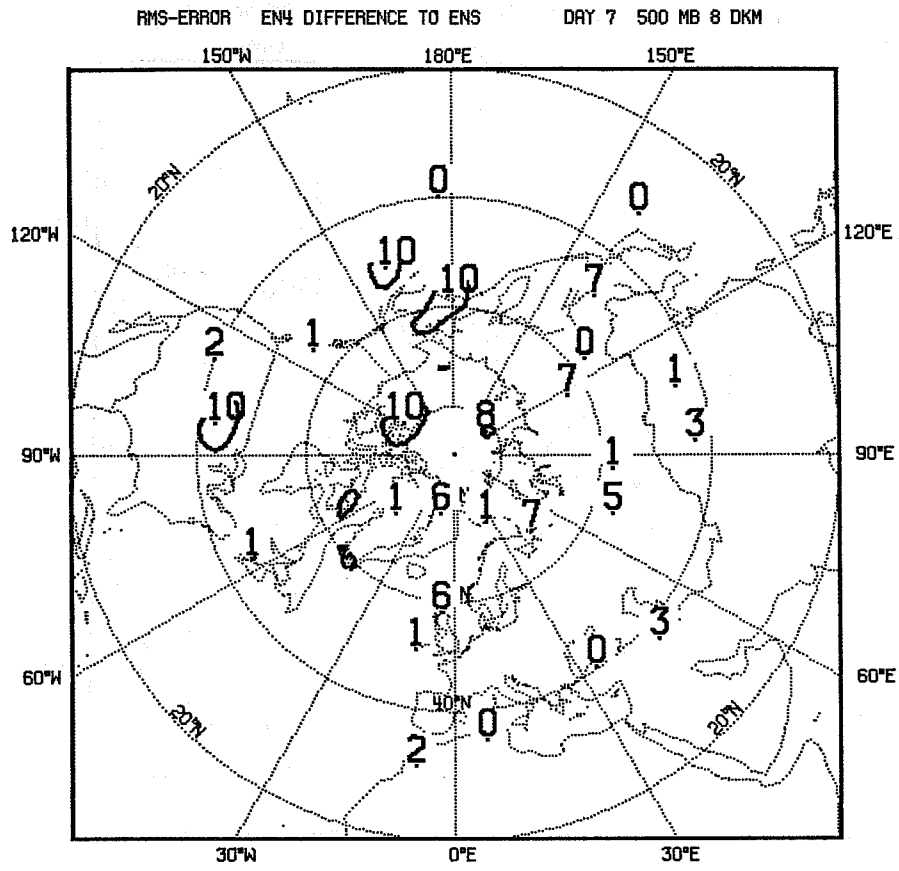

Fig. 9 As Fig. 8 at day 7

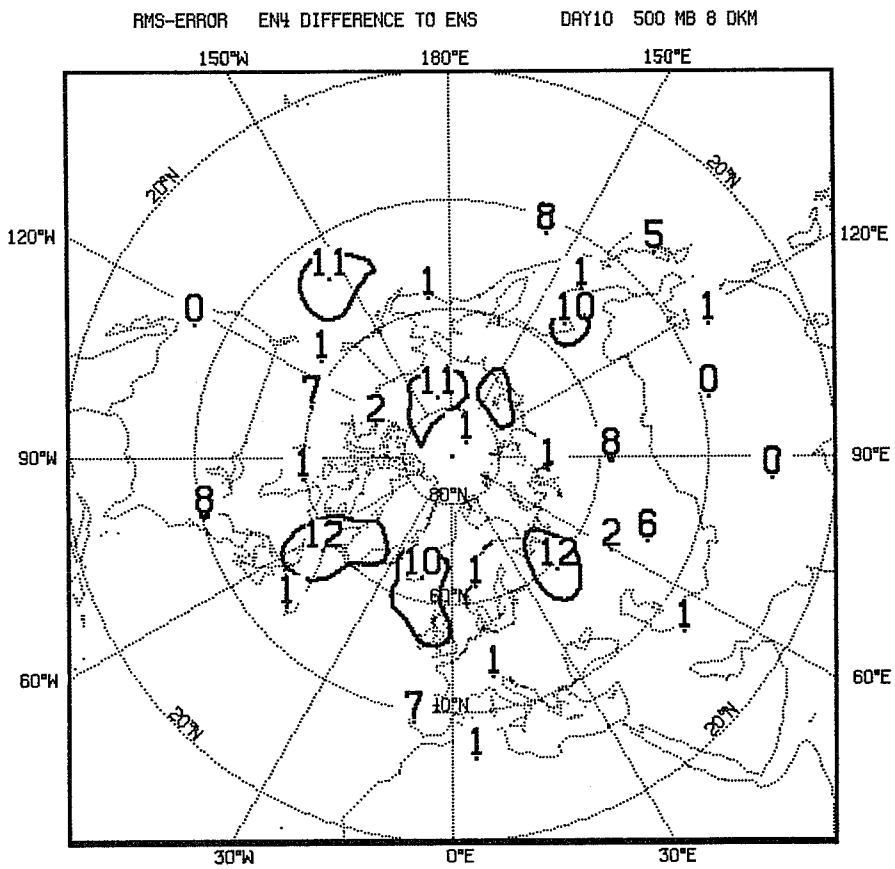

Fig. 10 As Fig. 8 at day 10

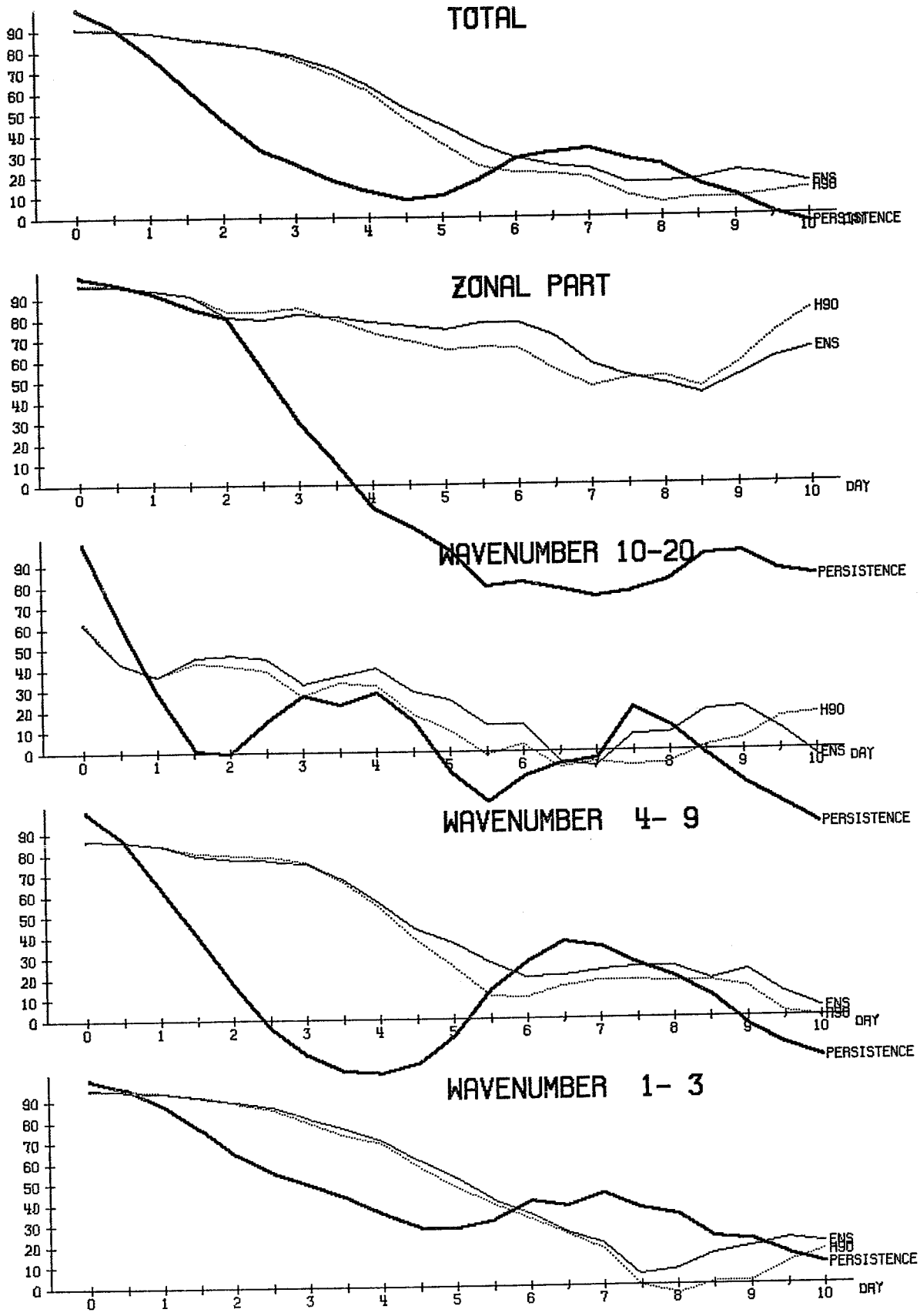

Fig. 11 Time evolution of the vertically averaged (200 mb - 1000 mb) and horizontally averaged (north of 20 N) RMS errors of persistence (thick line), control forecast (dotted line) and the ensemble mean forecast (thin line). The horizontal line marked NORM is the level of the climatological variance.

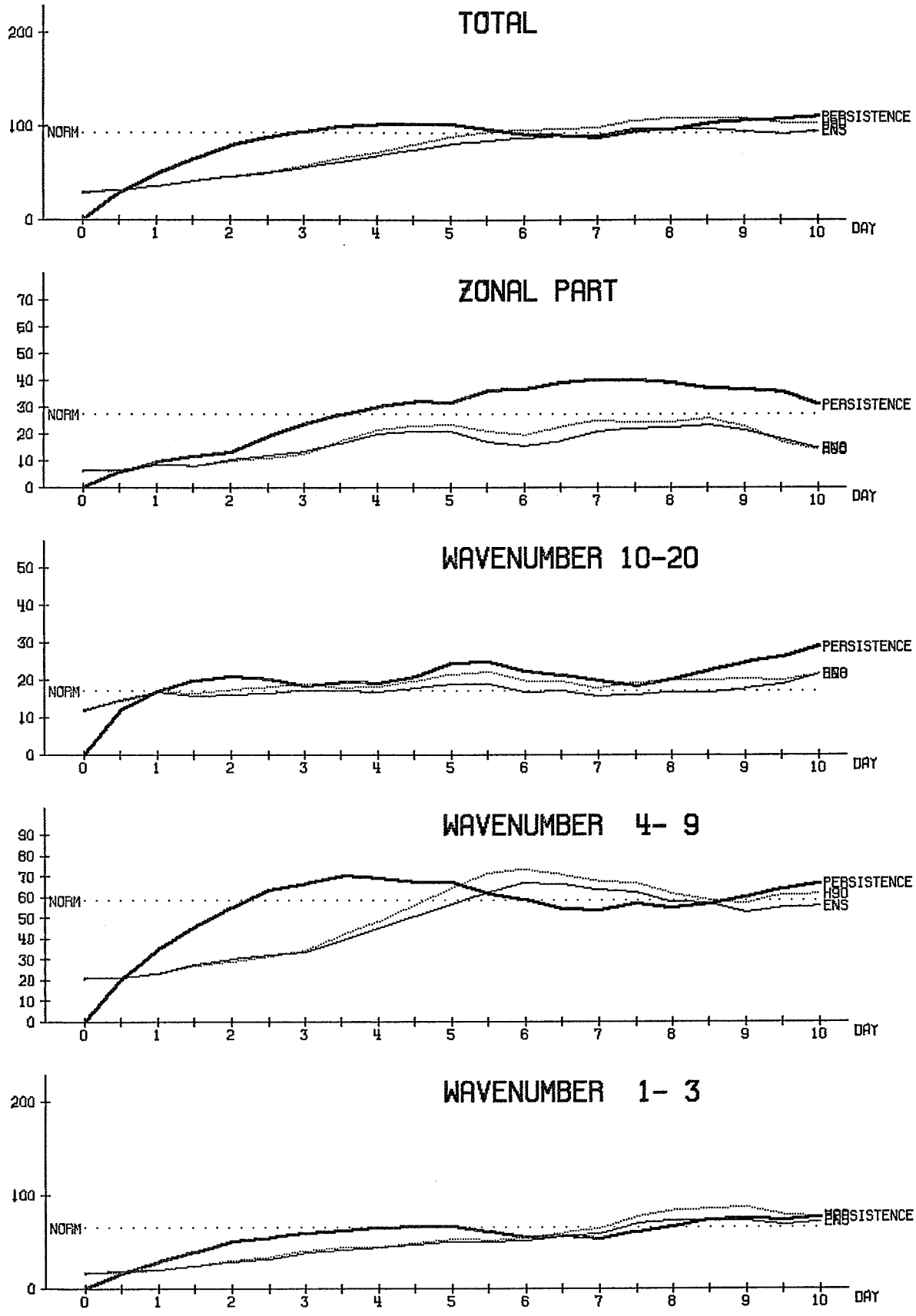

Fig. 12 As Fig. 11 for the anomaly correlation coefficient

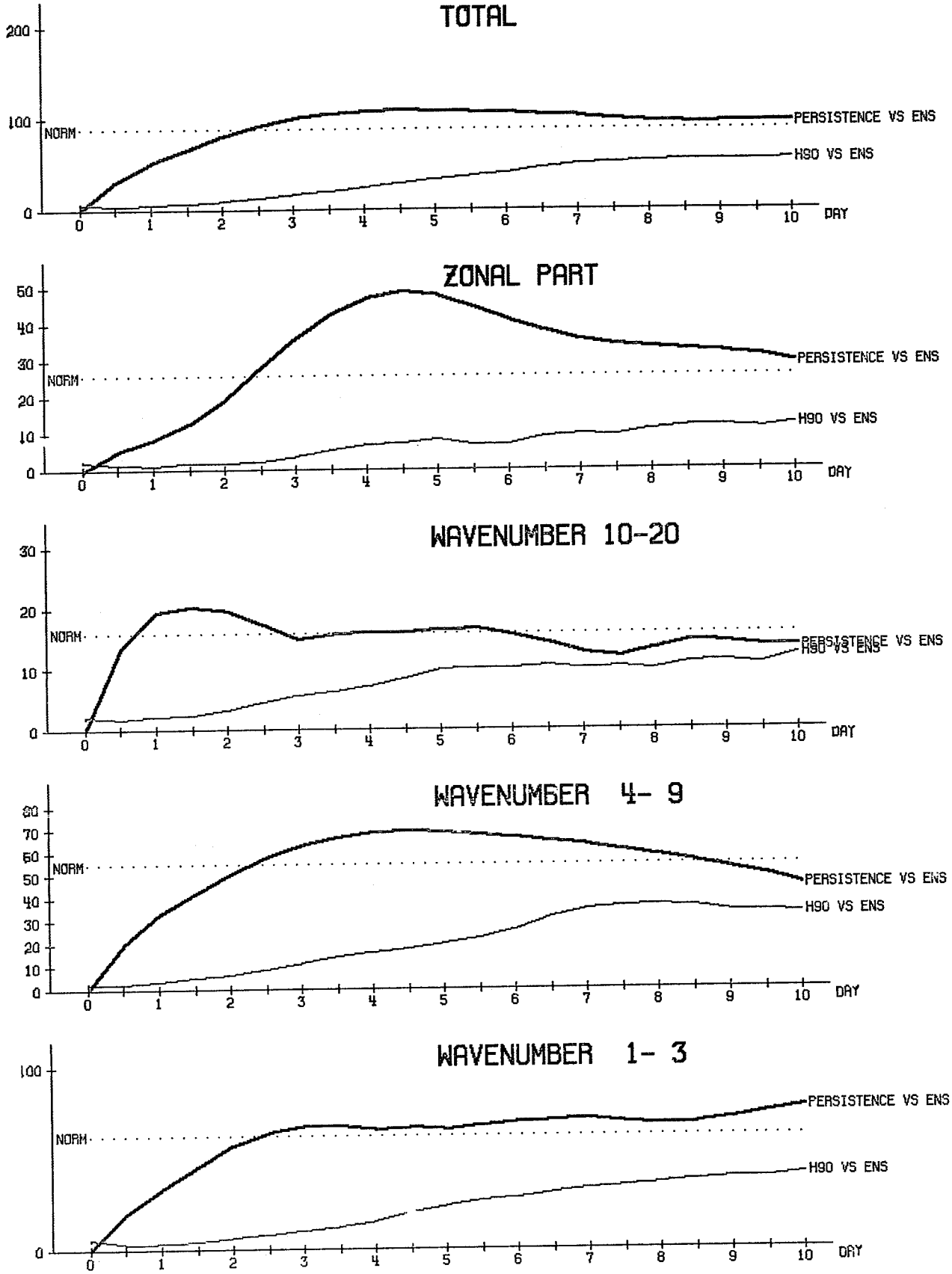

Fig. 13 Time evolution of the horizontally averaged (north of 20 N) RMS differences in 500 mb height between persistence and ensemble mean (thick line) and between the control forecast and ensemble mean (thin line).

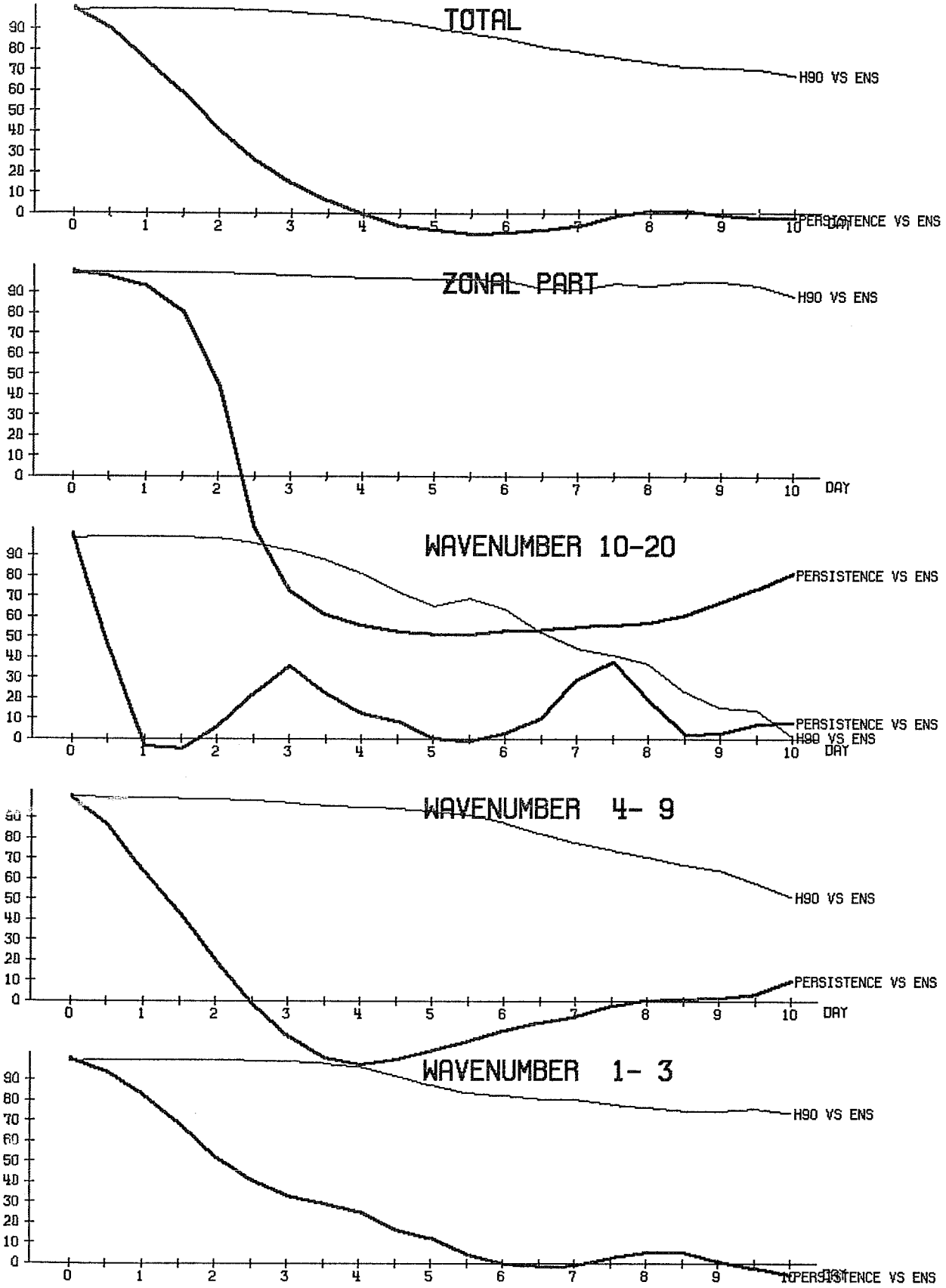

Fig. 14 As Fig. 13 for the anomaly correlation.